24th COBEM - 2017

24th ABCM International Congress of Mechanical Engineering
December 3-8, 2017, Curitiba, PR, Brazil

COBEM-2017-1332
EFFECTS OF LINEAR RESONATORS ON THE AEROELASTIC BEHAVIOR OF A PLATE-LIKE WING

João Henrique Ribeiro Dainezi
Carlos De Marqui Junior
USP - University of São Paulo, São Carlos School of Engineering - EESC, Avenida Trabalhador Sancarlense 400, Centro, São Carlos - SP
joao.dainezi@usp.br, demarqui@sc.usp.br

Abstract. *Metamaterials are a class of material with properties that do not occur naturally or are not obtained from their constituent materials. In this work, the effects of an array of linear resonators (locally resonant metamaterial) on the mechanical and aeromechanical behavior of a plate-like wing model are investigated. Finite element simulations are performed using the commercial software Nastran along with a self-developed continuous model of a plate. In both cases, the unsteady aerodynamic loads are obtained from the doublet lattice method. The bandgap created by the presence of the array of resonators is compared to theoretical predictions recently discussed in the literature and its consequence to the system aeroelastic behavior is analyzed.*

Keywords: *Aeroelasticity, Resonant Metamaterial, Bandgap, Unsteady Aerodynamics*

1. INTRODUCTION

In this work, the effects of resonant metamaterials - materials with properties that do not occur naturally or are not obtained from their constituent materials (Pendry *et al.*, 1999) - on the behavior of a flexible plate is investigated. An important characteristic of elastic/acoustic metamaterials is their ability to tailor the propagation of elastic waves through the generation of bandgaps. Bandgaps are frequency ranges of substantial wave attenuation due to wave scattering at periodic impedance mismatch zones (Bragg scattering) (Kittel and Holcomb, 1967) or are generated by distributed resonating units (Liu *et al.*, 2000). Bragg scattering bandgaps occur at wavelengths of the order of the unit cell size and they have been successfully exploited in phononic crystals to filter, localize, and guide acoustic waves (Hirsekorn *et al.*, 2006; Oudich *et al.*, 2011). Locally resonant metamaterials are capable of producing frequency attenuation regions that are not dependent of the latticed constant defining the spatial distribution of the resonators. Therefore, locally resonant metamaterials are able to generate low frequency attenuation zones (Liu *et al.*, 2000), which have been primarily investigated for vibration and noise radiation control applications as well as frequency filtering, wave guiding, and negative refraction.

The literature includes configurations of acoustic metamaterials with discrete absorbers (resonators) dispersed periodically in a stiff matrix. Yao *et al.* (2008) investigate one-dimensional mass-spring system with negative effective mass and its anti-vibration applicability. Wang *et al.* (2004) investigate the effects of two-dimensional phonic crystals resonators on the behavior of composite structures. Sonic bandgap (high frequency) was succefully induced in an alluminium plate by Oudich *et al.* (2011). Several authors (Cui *et al.*, 2009; Xiao *et al.*, 2008; Still *et al.*, 2011; Hirsekorn *et al.*, 2006; Hsu and Wu, 2007), consider local ressonators of one or more degrees of freedom in their research as well as Helmoltz resonators in acoustic waveguide (Cheng *et al.*, 2008; Fang *et al.*, 2006). However, a challenge in acoustic/elastic metamaterials research field is the ability to tune their performance for specific frequencies without requiring microstructural modifications. An ideal case could be described as a metamaterial whose properties of the constituent materials could be chosen or modified in order to tailor the bandgap region. Nevertheless, actively modifying the bandgap frequency range is not practical for passive metamaterials, such as the locally resonant (mechanical) metamaterials, usually discussed in the literature. The use of large deformations (Bertoldi and Boyce, 2008) and electro/magneto-mechanical coupling (Airoldi and Ruzzene, 2011; Vasseur *et al.*, 2011) managed to control the bandgaps in recent studies.

The objective of the present work is to investigate the behavior of a locally resonant metamaterial immersed in an uniform airflow of constant speed. In a recent paper, Sugino *et al.* (2016) presents a novel argument and modeling for bandgap formation in finite-length locally resonant metamaterias. The model, which is used as the reference model in the present paper, is based on the modal analysis of a locally resonant metamaterial and on the assumption of infinitely resonators. Considering the interaction of elastic metamaterials with flow, Casadei and Bertoldi (2014) created a self-adaptative metamaterial with a periodic array of airfoil-shaped resonators attached to a flexible wing. Since the aeroelastic behavior of each aeroelastic typical section changes with airflow speed, the bandgap formation is also modified for each

flow speed considered in their investigation.

Although several types of aeroelastic phenomena have been investigated, flutter has received the most attention due to its destructive nature (Bisplinghoff *et al.*, 2013). Airplane manufacturers avoid flutter by increasing the structural stiffness or mass redistribution, both causing significant strucutural weight increment. In this research, the aeroelastic behaviour of a plate-like wing with an array of linear resonators will be numerically investigated. This preliminarily investigation will be later extended to different aeroelastic phenomena as well as to the use of nonlinear mechanical absorbers.

2. MODEL

This section describes the mathematical models considered in the numerical simulation.

2.1 Metamaterial modeling

The metamaterial investigated in this research consists of an aluminium rectangular plate with locally distributed linear mass-spring resonators. The dynamics of this set is modeled with simple action-reaction Newton law, by adding one extra line and column in the mass and stiffness matrix of the original system for each resonator included, and adding the correct interaction factors in the original matrix.

Equation (1) shows the governing equation of the plate and Eq. (2), the equation of the resonators.

$$D\left(\frac{\partial^4 w}{\partial x^4}+2\frac{\partial^4 w}{\partial x^2\partial y^2}+\frac{\partial^4 w}{\partial y^4}\right)-\sum_{j=1}^{S} m_j\omega_{a,j}^2 u_j(t)\delta(x-x_j,y-y_j)+m\frac{\partial^2 w}{\partial t^2}=f(x,y)-m\ddot{w}_b(t) \tag{1}$$

$$\ddot{u}_j(t)+\omega_{a,j}^2 u_j(t)+\frac{\partial^2 w}{\partial t^2}(x_j,y_j,t)=-\ddot{w}_b(t) \tag{2}$$

$$D=\frac{2h^3E}{3(1-\nu^2)} \tag{3}$$

where w represents the plate deformation, m_j is the mass, $\omega_{a,j}$ is the natural frequency and u_j is the relative displacement of resonator j. δ is the dirac delta, m is the mass per unit area of the plate, f is an external force which is the aerodynamic force, h is the plate thickness, E is the Young modulus and ν is the Poisson ratio.

The bandgap frequency width can be estimated for the pure mechanical behaviour assuming an infinite number of resonators uniformly distributed over the plate (Sugino *et al.*, 2016). Equation (4) shows the estimated bandgap width.

$$\Delta\omega=\omega_t\left(\sqrt{1+\mu}-1\right) \tag{4}$$

where μ is the ratio of total mass of resonators to the original structure mass and the target frequency of the resonators is given as,

$$\omega_t=\frac{2\omega_c}{1+\sqrt{1+\mu}} \tag{5}$$

and ω_c is the central frequency of the bandgap.

2.2 Structural and unsteady aerodynamic modeling

The plate structural model is build based on the analytical modes of a vibrating plate (Leissa, 1969) with the corresponding boundary condition (clamped at the root and free at the other edges). The aerodynamic model is the Doublet-Lattice Method (DLM) (Albano and Rodden, 1969), which calculates the aerodynamic influence of the panels considering a doublet line at the quarter chord of each one and its pressure disturbance at the collocation point, assumed at three quarters of the chord and mid-span. There is a simplification in the equations when all the panels are coplanar (Blair, 1992), resulting in

$$\bar{w}(x,y,0)=U\alpha, \tag{6}$$

$$\frac{\alpha}{\Delta p}=\left[\frac{-\Delta\xi}{4\pi\rho U^2}\right]\left[B_0+B_1+B_2\right], \tag{7}$$

$$AIC(k)=\frac{\alpha}{\Delta C_p}=\left[\frac{-1}{8\pi}\right]\left[B_0+B_1+B_2\right], \tag{8}$$

where AIC (Aerodynamic Influence Coefficient) matrix, relates the incidence with the change of pressure coefficient in each panel, U represents the free-stream velocity, $\bar{w}(x, y, 0)$ is the downwash at the collocation point located at (x,y,0), α is the panel incidence, ρ is the air density, $\Delta\xi$ is the panel mean chord, B_0, B_1, B_2 are geometry dependent parameters.

The coupling between the structural nodes and the aerodynamic control points is performed with an Infinite Plate Spline (IPS) (Harder and Desmarais, 1972).

Combining the data obtained from the modeling specified above, the generalized airforce matrix (GAF), that relates the modal displacements and the modal aerodynamic forces in the reduced frequency domain (NASA, 1981), is obtained as,

$$[GAF](k) = [\Phi^T][G_{SS}][AIC(k)]^{-1}\left([D1_{GG}] + ik[D2_{GG}]\right)[\Phi], \tag{9}$$

where Φ represents the modal shapes matrix, $D1_{GG}$ is the spline matrix relating the translation in the structural grids to the change of incidence in the aerodynamic panels, $D2_{GG}$ is the spline matrix relating the translation in the structural grids to the translation of the aerodynamic panels, G_{SS} is the transpose of $D2_{GG}$ multiplied by the area of each panel and $k = \frac{\omega b}{U}$ is the reduced frequency with b representing half of the mean aerodynamic chord.

The GAF is used in the frequency response function (FRF) and flutter PK-method (Hassig, 1971) calculations. The FRF is the ratio of amplitude of a reference point to the base motion amplitude obtained from

$$FRF(\omega) = \left|\frac{\sum_{i=1}^{N}\eta_i\phi_i(\mathbf{x_{ref}})}{\bar{w_b}}\right|, \tag{10}$$

$$\eta_i = \frac{\bar{w_b}\omega^2\int_0^{L_x}\int_0^{L_y}\phi_i(x,y)dydx}{(\omega_i^2-\omega^2)L_xL_y}, \tag{11}$$

where ϕ_i corresponds to the modal shape of mode i, $\mathbf{x_{ref}}$ are the coordinate points of the reference point where the FRF will be evaluated, L_x and L_y are the plate length in x and y direction, respectively, ω_i is the natural frequency of mode i, ω is the base motion frequency and $\bar{w_b}$ is the amlitude of the base motion.

The flutter solution technique employed is the modal PK-method (Van Zyl, 1993). The eigenvalue problem is summarized in Eq. (12), corresponding to the matricial form from Eq. (13) and (14). This system is solved iteratively, obtaining p (Eq. (15)) and k for each airflow speed and mode.

$$\left[p^2[M_{hh}] + p\left([C_{hh}] - \frac{\rho bU}{4}\frac{\mathbb{I}\mathrm{m}([GAF])}{k}\right) + [K_{hh}] - (\frac{\rho U^2}{2})\mathbb{I}\mathrm{Re}([GAF])\right]\{q\} = \{0\} \tag{12}$$

$$([A] - p[I])\{q\} = \{0\} \tag{13}$$

$$[A] = \begin{bmatrix} [0] & [I] \\ -[M_{hh}]^{-1}\left([K_{hh}] - \frac{1}{2}\rho U^2\mathbb{I}\mathrm{Re}([GAF])\right) & -[M_{hh}]^{-1}\left([C_{hh}] - \frac{1}{4}\rho Ub\frac{\mathbb{I}\mathrm{m}([GAF])}{k}\right) \end{bmatrix} \tag{14}$$

$$p = g + i\omega \tag{15}$$

The hh index represents a modal parameter, p is the eigenvalue and q is the eigenvector of $[A]$ matrix. The parameter g indicates instability when positive, ω is the damped natural frequency of the considered mode; M, C and K represent the structural mass, damping and stiffness parameters respectively. I is the identity matrix, ρ is the air density, U is the airflow speed, k is the reduced frequency and b is the reference lenght equals half of the mean aerodynamic chord.

Time solution of the vibrating system is obtained with an approximation of the aerodynamic influence coefficient matrix in the time domain with Roger's method (Roger, 1977) and a state-space time integrator. This analysis allowed a better motion visualisation and the outputs were considered for an energy investigation. The time solution is obtained from the state space ODE shown in Eq. (16).

$$\{\dot{X}\} = \begin{bmatrix} [0] & [I] & [0] \\ -\left[\bar{M}\right]^{-1}\left[[K_{hh}] - q_\infty\left[A_{hh0}\right]\right] & -\left[\bar{M}\right]^{-1}\left[[C_{hh}] - q_\infty\frac{b}{U}\left[A_{hh1}\right]\right] & q_\infty\left[\bar{M}\right]^{-1}[D] \\ [0] & [E_h] & \frac{U}{b}[R] \end{bmatrix}\{X\} + \{b_{hh}\} \tag{16}$$

$$\left[\bar{M}\right] = \left[[M_hh] - \frac{q_\infty b^2}{U^2}\left[A_hh2\right]\right] \tag{17}$$

$[A_{hh0}]$, $[A_{hh0}]$, $[A_{hh0}]$, $[R]$, $[E_h]$ and $[D]$ are matrices obtained from $[GAF]$ with Roger's approximation, b_{hh} is the modal input force vector and q_∞ is the dynamic pressure of the freestream.

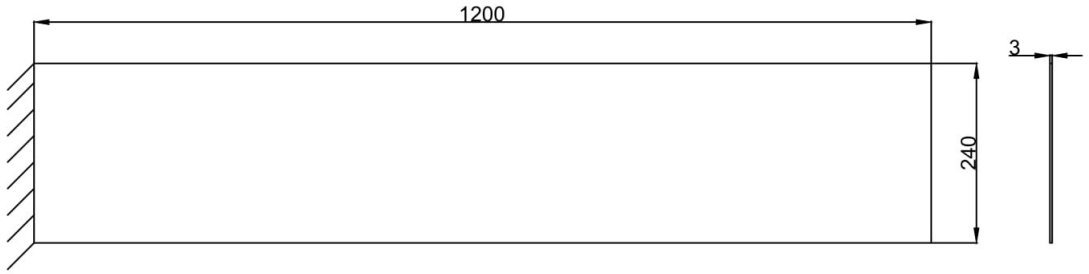

Figure 1. Dimensions in mm of the plate-like wing model

3. RESULTS

The simulations were performed considering an aluminium ($\rho = 2750kg/m^3$, $E = 70GPa$, $\nu = 0.3$) rectangular plate (1.2x0.24x0.003 m), as shown in Fig. 1, imersed in an uniform airflow. The clampled end of the plate can be connected to a shaker to introduce turbulence disturbances of a desired amplitude and frequency.

The aerodynamic mesh employed in the numerical analysis consists of 20 panels spanwise and 8 chordwise, considering half-span symmetry. The structural mesh contains 20 nodes spanwise and 9 chordwise. The metamaterial plate has 90 uniformly distributed resonators (10 spanwise and 9 chordwise) and the mass ratio to the original structure was set as $\mu = 0.7$ and the stiffness chosen in order to tune its natural frequency to create a bandgap at the flutter frequency of the plain plate. The modal analysis were performed with 6 modes in the plain plate and all modes with natural frequencies equal or below the 6^{th} mode frequency in the metamaterial plate. Figures 2 and 3 show the PK flutter analysis of the plain plate (without resonators). The linear flutter speed is $V = 69.4$ m/s and the flutter frequency is calculated as $f = 5.95$ Hz.

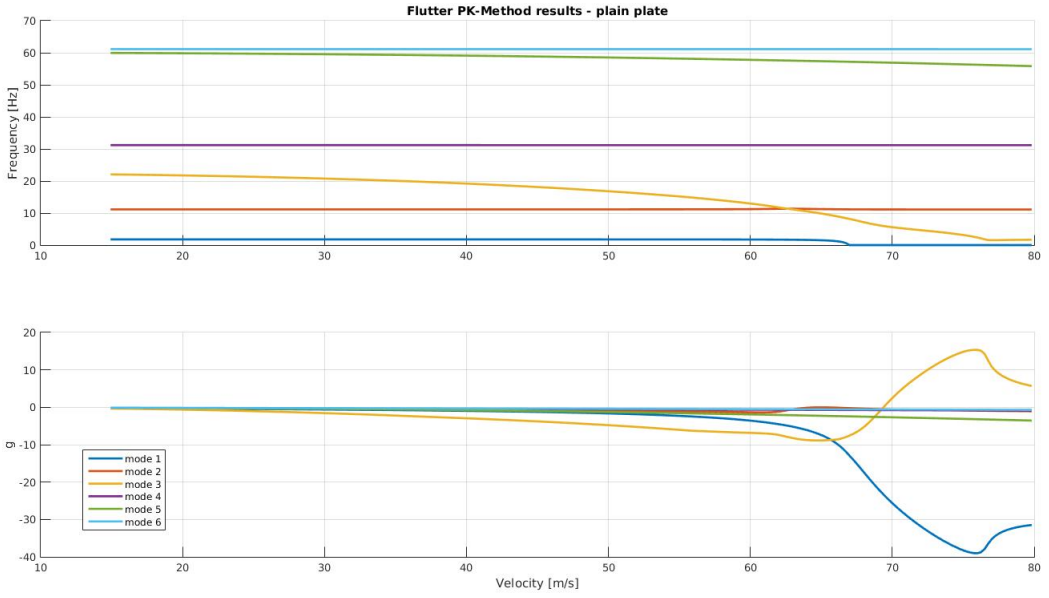

Figure 2. PK-method results of the plain plate

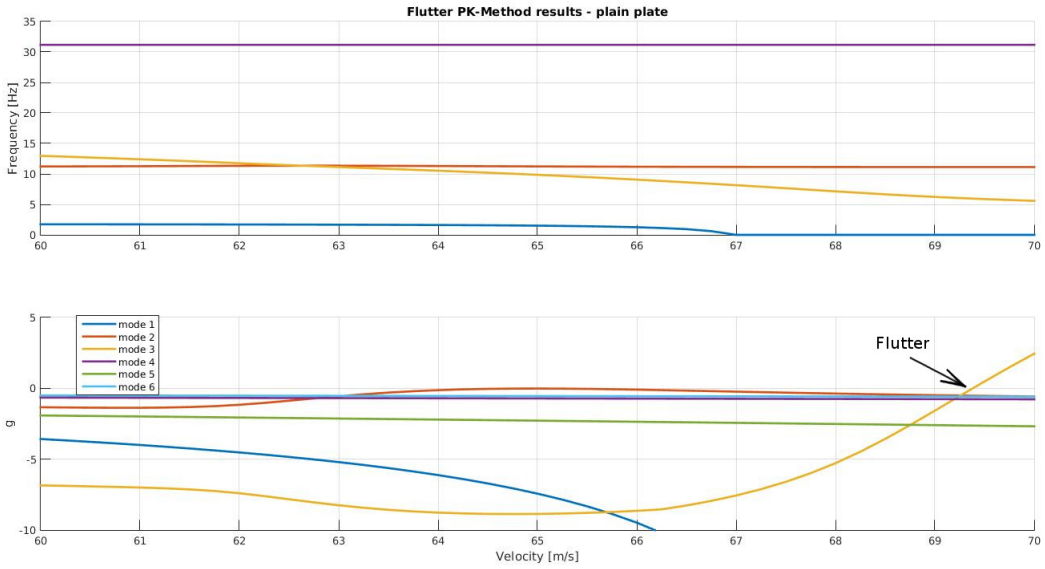

Figure 3. PK-method results of the plain plate - flutter detail

Having verified the aeroelastic behavior of the plain plate, the aeroelastic behavior of the metamaterial plate is now discussed. Figures 4 and 5 display the PK solution for the plate with an array of linear resonators. From the literature of flutter, it begins at $V = 60.3$ m/s and $f = 4.79$ Hz (mode 2), but it is a soft flutter, i.e. this mode becomes slightly unstable and returns to a stable state as speed increases. This kind of instability is easily controled with structural damping (not included in this simulation) and does not represent a serious threat. The significant instability occours at $V = 68.8$ m/s and $f = 4.77$ Hz (mode 3). The absorbers decreased the flutter speed and frequency.

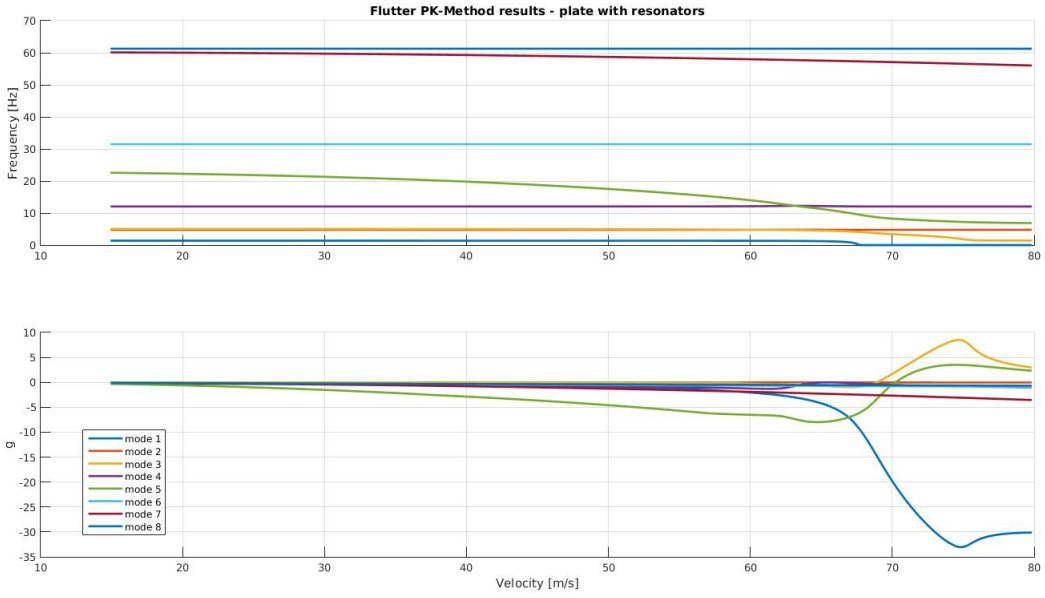

Figure 4. PK-method results of the metamaterial plate

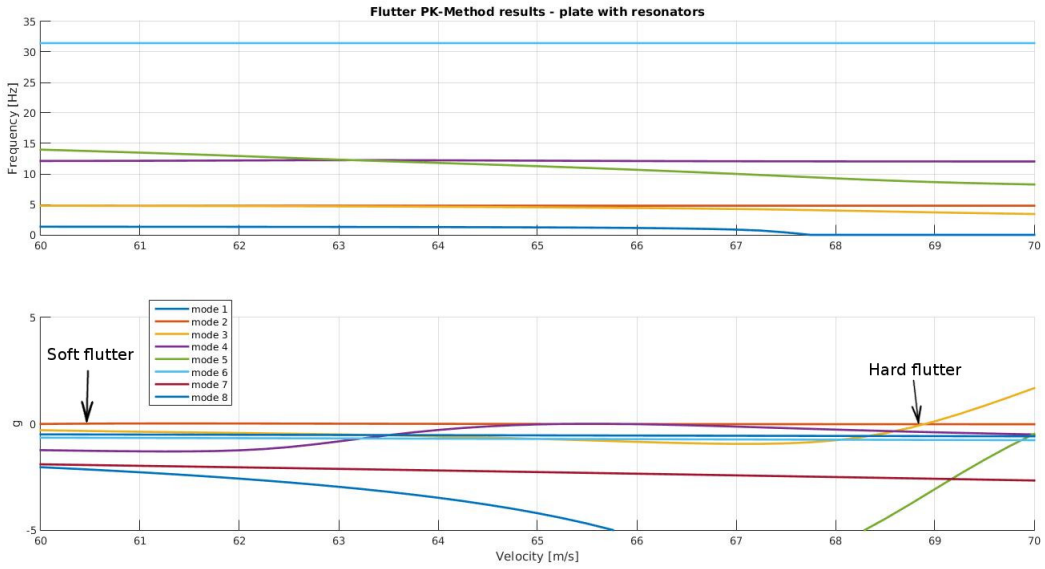

Figure 5. PK-method results of the metamaterial plate - flutter detail

Figures 6 and 7 show the heatmap of the plain plate and of the metamaterial plate, respectively, and the flutter speed is indicated in both cases. The heatamap shows the aeroelastic evolution with increasing airflow speed and also the bandgap obtained for the metamaterial plate. A good agreement can be seen between this results and the PK flutter analysis, the main difference consists of the abscence of the 3^{rd} mode in the FRF, wich corresponds to the torsional mode. Since harmonic base motion is uniform, then torsional modes are not expected to show in the heatmap at low flow speeds, but it appears at high speed, close to flutter, due to modal coupling.

The bandgap can be observed in Fig. 7, corresponding to the blue strip around 6 Hz. The bandwidth calculated from the heatmap is 1.617 Hz and 1.8 Hz when calculated form Eq. (4), showing good agreement between the infinite resonators theory and the numerical simulation performed. Wider bandgaps are expected for larger mass ratios (that are limited to 0.7 in the present work). Figure 8 shows the FRF for three cases: flutter of the plain plate, low flow speed from the plain plate and the resonant metamaterial. It can be seen that the bandgap is centered at the original plate flutter frequency and the introduction of resonators creates new peaks, marked with circles, at frequencies lower and higher than the bandgap limits. The first two new peaks are the ones causing the soft and hard flutter (Fig. 5 and 7), explaining why the flutter speed decreases with the inclusion of resonators.

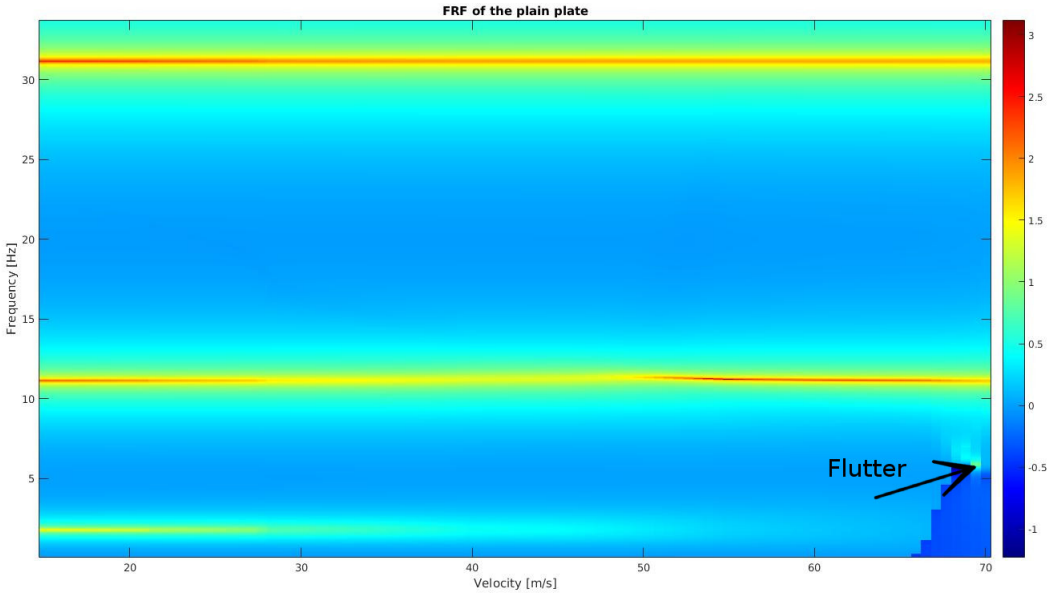

Figure 6. FRF heatmap for different frequencies and airflow speed - plain plate

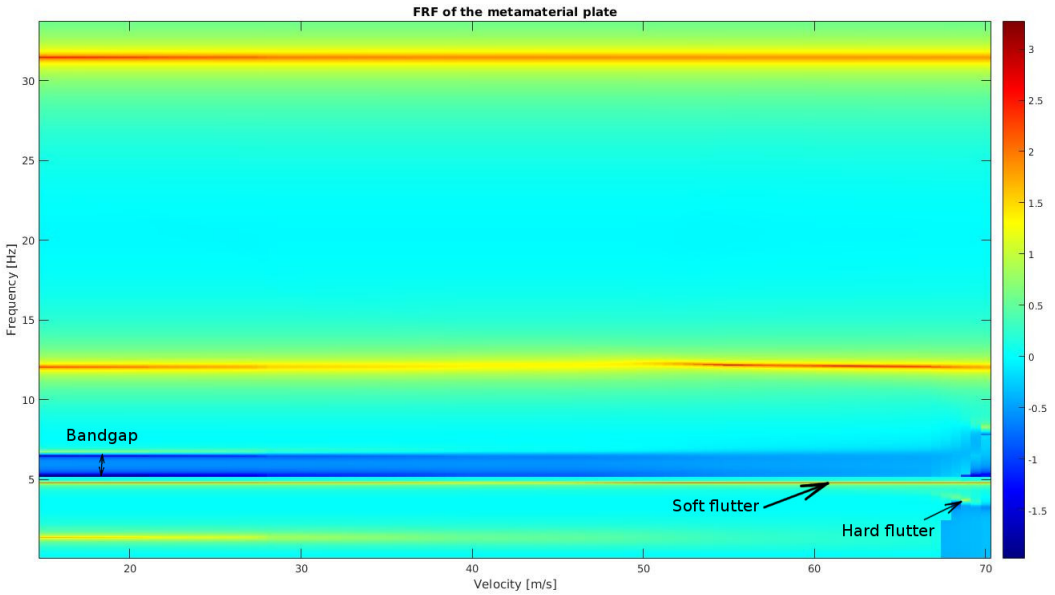

Figure 7. FRF heatmap for different frequencies and airflow speed - metamaterial plate

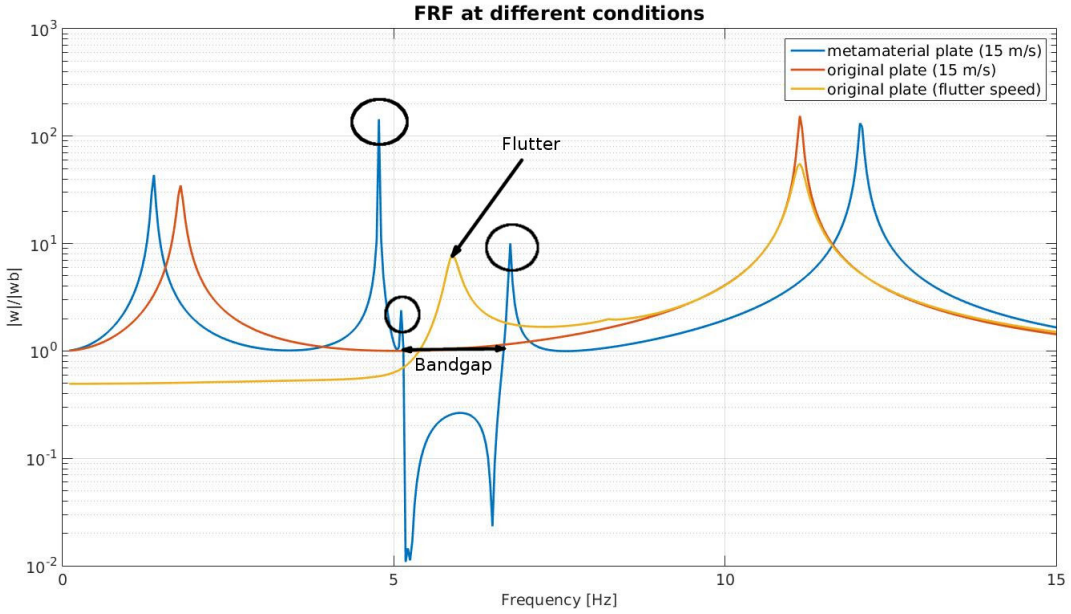

Figure 8. FRF comparison

Another investigation was conducted with an energy analysis in order to comprehend the metamaterial mechanical behavior. Figures 9 and 10 show the total energy of the system (potential elastic and kinetic) of the plate and the resonators with time in different conditions, first at a pure mechanical resonance (flow speed zero and base excitation frequency 1.4 Hz) and inside the bandgap (flow speed zero and base excitation frequency 5.2 Hz) up to 40 seconds.

In Fig. 10 it can be seen that inside the bandgap the amount of energy on the plate is minimum compared to the resonators, showing that in this condition the resonators absorb most of the system energy and the system energy level is limited to a finite band, showing stability. Figure 9 compares the energy of plate and resonators in the first mechanical ressonance, showing that the plate contains more energy than the resonators. In this case the total energy grows constantly, corresponding to an unstable condition. The kinetic energy is shown for the same two cases up to 1 second in Fig. 11 and 12. At the resonance, the kinetic energy of the plate and the resonators are in phase, while inside the bandgap there is a difference of approximately $\frac{\pi}{2}$ radians. This difference in phase is a consequence of the resonators operation principle: the relative motion between the plate and the resonators creates a force in opposition to the plate movement tendency,

canceling the vibration. During flutter (flow speed 68.8 m/s and base excitation frequency 4.8 Hz) energy grows so quickly that the simulation achieves overflow in 0.16 seconds of simulation. The structure is accumulating energy from the flow and is not able to dissipate it due to the abscence of damping in the model.

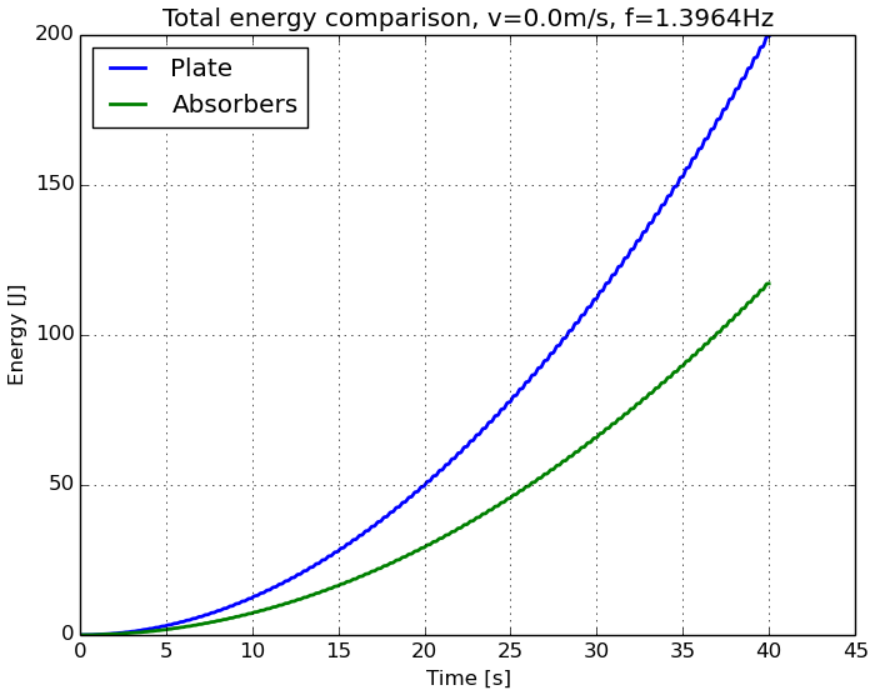

Figure 9. Total Energy comparison during first resonance

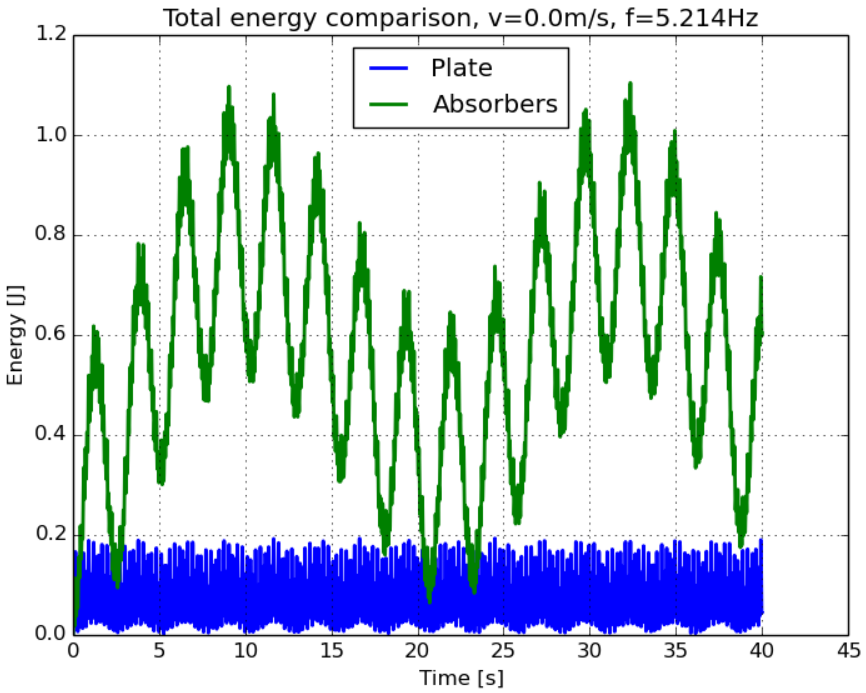

Figure 10. Total Energy comparison inside the bandgap

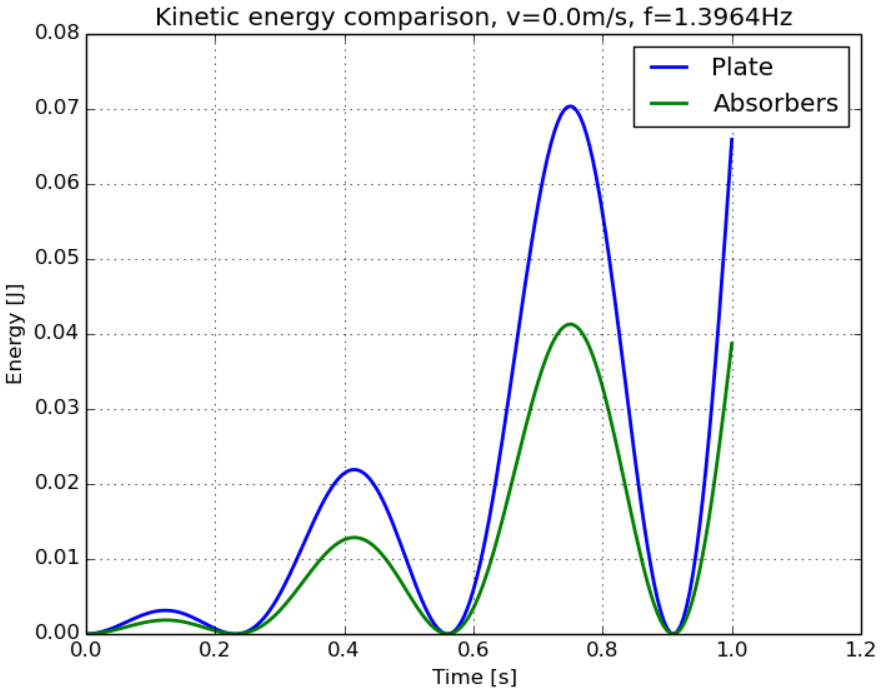

Figure 11. Kinetic Energy comparison during first resonance

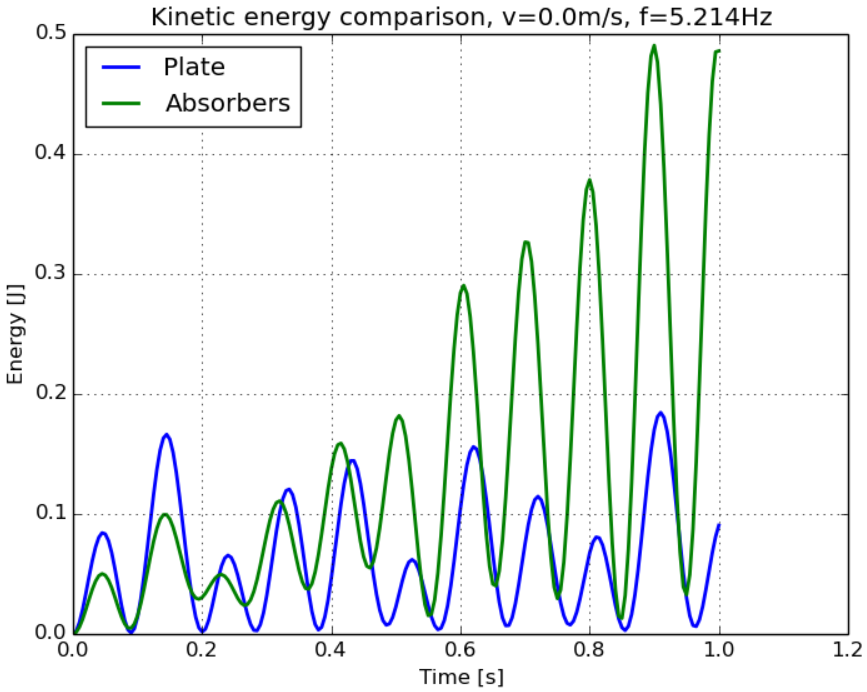

Figure 12. Kinetic Energy comparison inside the bandgap

4. CONCLUSION

Although metamaterial with linear mass-spring local resonating units have proved eficient to absorb energy in mechanical systems, the same conclusion cannot be achived for aeroelastic systems. The amount of energy introduced by the airflow grows exponentialy when flutter occours, which cannot be totally absorbed by the resonators. The side effect of the resonators inclusion is the creation of new resonances, which is not a problem in pure mechanical systems where

there is no modal coupling due to aerodynamic effects. Damping should be necessary in order to the resonator eliminate the extra energy and this configuration will be investigated further in a future resarch.

5. ACKNOWLEDGEMENTS

We thank FAPESP (Fundação de Amparo à Pesquisa do Estado de São Paulo) for the financial suport of this research, FAPESP file 2016/20841-8.

6. REFERENCES

Airoldi, L. and Ruzzene, M., 2011. "Design of tunable acoustic metamaterials through periodic arrays of resonant shunted piezos". *New Journal of Physics*, Vol. 13, No. 11, p. 113010.

Albano, E. and Rodden, W.P., 1969. "A doublet-lattice method for calculating lift distributions on oscillating surfaces in subsonic flows." *AIAA journal*, Vol. 7, No. 2, pp. 279–285.

Bertoldi, K. and Boyce, M., 2008. "Mechanically triggered transformations of phononic band gaps in periodic elastomeric structures". *Physical Review B*, Vol. 77, No. 5, p. 052105.

Bisplinghoff, R.L., Ashley, H. and Halfman, R.L., 2013. *Aeroelasticity*. Courier Corporation.

Blair, M., 1992. "A compilation of the mathematics leading to the doublet lattice method". Technical report, WRIGHT LAB WRIGHT-PATTERSON AFB OH.

Casadei, F. and Bertoldi, K., 2014. "Harnessing fluid-structure interactions to design self-regulating acoustic metamaterials". *Journal of Applied Physics*, Vol. 115, No. 3, p. 034907.

Cheng, Y., Xu, J. and Liu, X., 2008. "One-dimensional structured ultrasonic metamaterials with simultaneously negative dynamic density and modulus". *Physical Review B*, Vol. 77, No. 4, p. 045134.

Cui, Z.Y., Chen, T.N., Chen, H.L. and Su, Y.P., 2009. "Experimental and calculated research on a large band gap constituting of tubes with periodic narrow slits". *Applied Acoustics*, Vol. 70, No. 8, pp. 1087–1093.

Fang, N., Xi, D., Xu, J., Ambati, M., Srituravanich, W., Sun, C. and Zhang, X., 2006. "Ultrasonic metamaterials with negative modulus". *Nature materials*, Vol. 5, No. 6, pp. 452–456.

Harder, R.L. and Desmarais, R.N., 1972. "Interpolation using surface splines." *Journal of aircraft*, Vol. 9, No. 2, pp. 189–191.

Hassig, H.J., 1971. "An approximate true damping solution of the flutter equation by determinant iteration". *Journal of Aircraft*, Vol. 8, No. 11, pp. 885–889.

Hirsekorn, M., Delsanto, P.P., Leung, A.C. and Matic, P., 2006. "Elastic wave propagation in locally resonant sonic material: Comparison between local interaction simulation approach and modal analysis". *Journal of applied physics*, Vol. 99, No. 12, p. 124912.

Hsu, J.C. and Wu, T.T., 2007. "Lamb waves in binary locally resonant phononic plates with two-dimensional lattices". *Applied physics letters*, Vol. 90, No. 20, p. 201904.

Kittel, C. and Holcomb, D.F., 1967. "Introduction to solid state physics". *American Journal of Physics*, Vol. 35, No. 6, pp. 547–548.

Leissa, A.W., 1969. "Vibration of plates". Technical report, OHIO STATE UNIV COLUMBUS.

Liu, Z., Zhang, X., Mao, Y., Zhu, Y., Yang, Z., Chan, C.T. and Sheng, P., 2000. "Locally resonant sonic materials". *science*, Vol. 289, No. 5485, pp. 1734–1736.

NASA, 1981. "The nastran theoretical manual. nasa sp-221(06)". Technical report, National Aeronautics and Space Administration.

Oudich, M., Senesi, M., Assouar, M.B., Ruzenne, M., Sun, J.H., Vincent, B., Hou, Z. and Wu, T.T., 2011. "Experimental evidence of locally resonant sonic band gap in two-dimensional phononic stubbed plates". *Physical Review B*, Vol. 84, No. 16, p. 165136.

Pendry, J.B., Holden, A.J., Robbins, D. and Stewart, W., 1999. "Magnetism from conductors and enhanced nonlinear phenomena". *IEEE transactions on microwave theory and techniques*, Vol. 47, No. 11, pp. 2075–2084.

Roger, K.L., 1977. "Airplane math modeling methods for active control design". *AGARD-CP-228*, pp. 4–1.

Still, T., Gantzounis, G., Kiefer, D., Hellmann, G., Sainidou, R., Fytas, G. and Stefanou, N., 2011. "Collective hypersonic excitations in strongly multiple scattering colloids". *Physical review letters*, Vol. 106, No. 17, p. 175505.

Sugino, C., Leadenham, S., Ruzzene, M. and Erturk, A., 2016. "On the mechanism of bandgap formation in locally resonant finite elastic metamaterials". *Journal of Applied Physics*, Vol. 120, No. 13, p. 134501.

Van Zyl, L.H., 1993. "Use of eigenvectors in the solution of the flutter equation". *Journal of aircraft*, Vol. 30, pp. 553–553.

Vasseur, J., Matar, O.B., Robillard, J., Hladky-Hennion, A.C. and Deymier, P.A., 2011. "Band structures tunability of bulk 2d phononic crystals made of magneto-elastic materials". *AIP advances*, Vol. 1, No. 4, p. 041904.

Wang, G., Wen, X., Wen, J., Shao, L. and Liu, Y., 2004. "Two-dimensional locally resonant phononic crystals with binary structures". *Physical review letters*, Vol. 93, No. 15, p. 154302.

Xiao, W., Zeng, G. and Cheng, Y., 2008. "Flexural vibration band gaps in a thin plate containing a periodic array of

hemmed discs". *Applied Acoustics*, Vol. 69, No. 3, pp. 255–261.

Yao, S., Zhou, X. and Hu, G., 2008. "Experimental study on negative effective mass in a 1d mass–spring system". *New Journal of Physics*, Vol. 10, No. 4, p. 043020.

7. RESPONSIBILITY NOTICE

The authors are the only responsible for the printed material included in this paper.